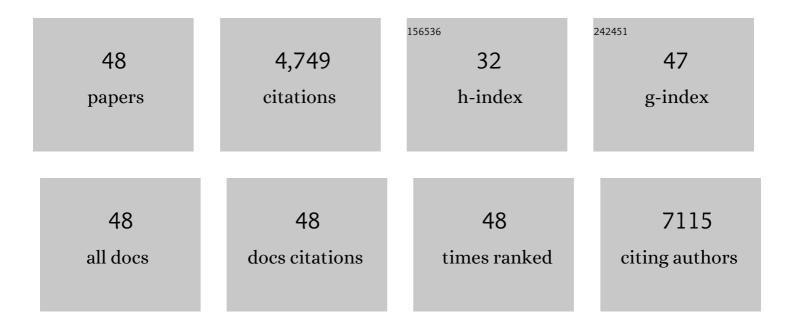


## List of Publications by Year in descending order

Source: https://exaly.com/author-pdf/6088977/publications.pdf Version: 2024-02-01



OIANG LL

#	Article	IF	CITATIONS
1	Support-based modulation strategies in single-atom catalysts for electrochemical CO <sub>2</sub> reduction: graphene and conjugated macrocyclic complexes. Journal of Materials Chemistry A, 2022, 10, 5699-5716.	5.2	13
2	Double-edged roles of intrinsic defects in two-dimensional MoS2. Trends in Chemistry, 2022, 4, 451-463.	4.4	5
3	A Universal Descriptor for Complicated Interfacial Effects on Electrochemical Reduction Reactions. Journal of the American Chemical Society, 2022, 144, 12874-12883.	6.6	49
4	Selective visible-light driven highly efficient photocatalytic reduction of CO <sub>2</sub> to C <sub>2</sub> H <sub>5</sub> OH by two-dimensional Cu <sub>2</sub> S monolayers. Nanoscale Horizons, 2021, 6, 661-668.	4.1	15
5	A new nitrogen fixation strategy: the direct formation of *N <sub>2</sub> <sup>â^'</sup> excited state on metal-free photocatalyst. Journal of Materials Chemistry A, 2021, 9, 6214-6222.	5.2	8
6	Promoting the conversion of CO <sub>2</sub> to CH <sub>4</sub> <i>via</i> synergistic dual active sites. Nanoscale, 2021, 13, 12233-12241.	2.8	16
7	Photocatalytic conversion of CO to fuels with water by B-doped graphene/g-C3N4 heterostructure. Science Bulletin, 2021, 66, 1186-1193.	4.3	19
8	Dynamic structure change of Cu nanoparticles on carbon supports for <scp>CO<sub>2</sub></scp> electroâ€reduction toward multicarbon products. InformaÄnÄ-Materiály, 2021, 3, 1285-1294.	8.5	22
9	Synergistic modulation of metal-free photocatalysts by the composition ratio change and heteroatom doping for overall water splitting. Journal of Materials Chemistry A, 2021, 9, 11753-11761.	5.2	14
10	Hybrid Cu <sup>0</sup> and Cu <i><sup>x</sup></i> <sup>+</sup> as Atomic Interfaces Promote Highâ€Selectivity Conversion of CO <sub>2</sub> to C <sub>2</sub> H <sub>5</sub> OH at Low Potential. Small, 2020, 16, e1901981.	5.2	92
11	Edge promotion and basal plane activation of MoS2 catalyst by isolated Co atoms for hydrodesulfurization and hydrodenitrogenation. Catalysis Today, 2020, 350, 56-63.	2.2	5
12	Metal single-atom coordinated graphitic carbon nitride as an efficient catalyst for CO oxidation. Nanoscale, 2020, 12, 364-371.	2.8	59
13	Breaking scaling relations for efficient CO <sub>2</sub> electrochemical reduction through dual-atom catalysts. Chemical Science, 2020, 11, 1807-1813.	3.7	230
14	Highly Efficient Photo-/Electrocatalytic Reduction of Nitrogen into Ammonia by Dual-Metal Sites. ACS Central Science, 2020, 6, 1762-1771.	5.3	135
15	Perspective on theoretical methods and modeling relating to electro-catalysis processes. Chemical Communications, 2020, 56, 9937-9949.	2.2	52
16	Unveiling chemical reactivity and oxidation of 1T-phased group VI disulfides. Physical Chemistry Chemical Physics, 2019, 21, 17010-17017.	1.3	7
17	Rational Design of Crystalline Covalent Organic Frameworks for Efficient CO <sub>2</sub> Photoreduction with H <sub>2</sub> O. Angewandte Chemie - International Edition, 2019, 58, 12392-12397.	7.2	360
18	Rational Design of Crystalline Covalent Organic Frameworks for Efficient CO <sub>2</sub> Photoreduction with H <sub>2</sub> 0. Angewandte Chemie, 2019, 131, 12522-12527.	1.6	88

Qiang Li

#	Article	IF	CITATIONS
19	New Mechanism for N <sub>2</sub> Reduction: The Essential Role of Surface Hydrogenation. Journal of the American Chemical Society, 2019, 141, 18264-18270.	6.6	166
20	Photo-oxidative degradation of methylammonium lead iodide perovskite: mechanism and protection. Journal of Materials Chemistry A, 2019, 7, 2275-2282.	5.2	105
21	Recent advances in oxidation and degradation mechanisms of ultrathin 2D materials under ambient conditions and their passivation strategies. Journal of Materials Chemistry A, 2019, 7, 4291-4312.	5.2	158
22	Metal-free electrocatalyst for reducing nitrogen to ammonia using a Lewis acid pair. Journal of Materials Chemistry A, 2019, 7, 4865-4871.	5.2	115
23	Degenerate electron-doping in two-dimensional tungsten diselenide with a dimeric organometallic reductant. Materials Today, 2019, 30, 26-33.	8.3	14
24	Installing earth-abundant metal active centers to covalent organic frameworks for efficient heterogeneous photocatalytic CO2 reduction. Applied Catalysis B: Environmental, 2019, 254, 624-633.	10.8	212
25	Role of Water and Defects in Photoâ€Oxidative Degradation of Methylammonium Lead Iodide Perovskite. Small Methods, 2019, 3, 1900154.	4.6	49
26	A General Two‣tep Strategy–Based Highâ€Throughput Screening of Single Atom Catalysts for Nitrogen Fixation. Small Methods, 2019, 3, 1800376.	4.6	303
27	Forming Atom–Vacancy Interface on the MoS 2 Catalyst for Efficient Hydrodeoxygenation Reactions. Small Methods, 2019, 3, 1800315.	4.6	23
28	On-surface synthesis: a promising strategy toward the encapsulation of air unstable ultra-thin 2D materials. Nanoscale, 2018, 10, 3799-3804.	2.8	18
29	Molybdenum sulfide clusters immobilized on defective graphene: a stable catalyst for the hydrogen evolution reaction. Journal of Materials Chemistry A, 2018, 6, 2289-2294.	5.2	44
30	Controllable etching of MoS2 basal planes for enhanced hydrogen evolution through the formation of active edge sites. Nano Energy, 2018, 49, 634-643.	8.2	220
31	Metal-Free Single Atom Catalyst for N <sub>2</sub> Fixation Driven by Visible Light. Journal of the American Chemical Society, 2018, 140, 14161-14168.	6.6	742
32	Computation-Aided Design of Single-Atom Catalysts for One-Pot CO <sub>2</sub> Capture, Activation, and Conversion. ACS Applied Materials & Interfaces, 2018, 10, 36866-36872.	4.0	70
33	Black Phosphorus: Abnormal Near-Infrared Absorption in 2D Black Phosphorus Induced by Ag Nanoclusters Surface Functionalization (Adv. Mater. 43/2018). Advanced Materials, 2018, 30, 1870325.	11.1	0
34	Insight into the catalytic activity of MXenes for hydrogen evolution reaction. Science Bulletin, 2018, 63, 1397-1403.	4.3	61
35	Abnormal Nearâ€Infrared Absorption in 2D Black Phosphorus Induced by Ag Nanoclusters Surface Functionalization. Advanced Materials, 2018, 30, e1801931.	11.1	43
36	Accelerated discovery of stable lead-free hybrid organic-inorganic perovskites via machine learning. Nature Communications, 2018, 9, 3405.	5.8	442

Qiang Li

#	Article	IF	CITATIONS
37	Photo-oxidative Degradation and Protection Mechanism of Black Phosphorus: Insights from Ultrafast Dynamics. Journal of Physical Chemistry Letters, 2018, 9, 5034-5039.	2.1	45
38	Effect of illumination and Se vacancies on fast oxidation of ultrathin gallium selenide. Nanoscale, 2018, 10, 12180-12186.	2.8	37
39	Waterâ€Catalyzed Oxidation of Few‣ayer Black Phosphorous in a Dark Environment. Angewandte Chemie - International Edition, 2017, 56, 9131-9135.	7.2	141
40	Passivation of Black Phosphorus via Selfâ€Assembled Organic Monolayers by van der Waals Epitaxy. Advanced Materials, 2017, 29, 1603990.	11.1	113
41	Band-edge engineering via molecule intercalation: a new strategy to improve stability of few-layer black phosphorus. Physical Chemistry Chemical Physics, 2017, 19, 29232-29236.	1.3	10
42	Nanoconfined Iron Oxychloride Material as a High-Performance Cathode for Rechargeable Chloride Ion Batteries. ACS Energy Letters, 2017, 2, 2341-2348.	8.8	87
43	Exploitation of the Largeâ€Area Basal Plane of MoS <sub>2</sub> and Preparation of Bifunctional Catalysts through Onâ€Surface Selfâ€Assembly. Advanced Science, 2017, 4, 1700356.	5.6	9
44	Towards a Comprehensive Understanding of the Reaction Mechanisms Between Defective MoS <sub>2</sub> and Thiol Molecules. Angewandte Chemie - International Edition, 2017, 56, 10501-10505.	7.2	88
45	Oxidation Mechanism and Protection Strategy of Ultrathin Indium Selenide: Insight from Theory. Journal of Physical Chemistry Letters, 2017, 8, 4368-4373.	2.1	62
46	Carbon incorporation effects and reaction mechanism of FeOCl cathode materials for chloride ion batteries. Scientific Reports, 2016, 6, 19448.	1.6	43
47	Covalent Functionalization of Black Phosphorus from First-Principles. Journal of Physical Chemistry Letters, 2016, 7, 4540-4546.	2.1	71
48	Magnesium Anode for Chloride Ion Batteries. ACS Applied Materials & Interfaces, 2014, 6, 10997-11000.	4.0	69